Simulation of Robotic Systems

Comparative Numerical Analysis of Integration Methods for Rotational Mass-Spring-Damper Systems

Oyetunde Jamiu Olaide
Student ID: 520194
Robotic and Artificial Intelligence

Simulation of Robotic Systems

ITMO University

St. Petersburg, Russia

Comparative Numerical Analysis of Integration Methods for Rotational Mass-Spring-Damper Systems

Introduction

Numerical integration of ordinary differential equations is essential for simulating dynamical systems in engineering. While analytical solutions exist for linear second-order systems, practical applications often involve more complex scenarios requiring computational approaches. This study investigates the performance of three numerical integration methods—Explicit Euler, Implicit Euler, and fourth-order Runge-Kutta—for solving the rotational mass-spring-damper system governed by the equation:

$$I\ddot{\theta} + b\dot{\theta} + (mgl + k)\theta = 0 \tag{1}$$

where $I = 0.08$ kgm^2, $b = 0.05$ Nms/rad, $m = 0.5$ kg, $g = 9.81$ m/s^2, $l = 0.3$ m, and $k = 9.4$ N/m. The initial conditions are $\theta(0) = 0.45$ rad and $\dot{\theta}(0) = 0$ rad/s. These parameters correspond to a specific experimental configuration with $m = 0.5$ kg and $k = 9.4$ N/m.

The goal of this work is to compare the accuracy and stability of these methods over a simulation period of 10 seconds with a step size of 0.01 seconds. The results provide practical guidance for selecting integration schemes in engineering simulations where computational efficiency must be balanced with numerical precision.

1 Model and ODE

1.1 System Description

We consider a rotational mass-spring-damper system with moment of inertia I, torsional spring constant k, and rotational damping coefficient b. The generalized coordinate is the angular displacement $\theta(t)$ from the vertical equilibrium position. The system is subject to both elastic restoring torque and gravitational torque.

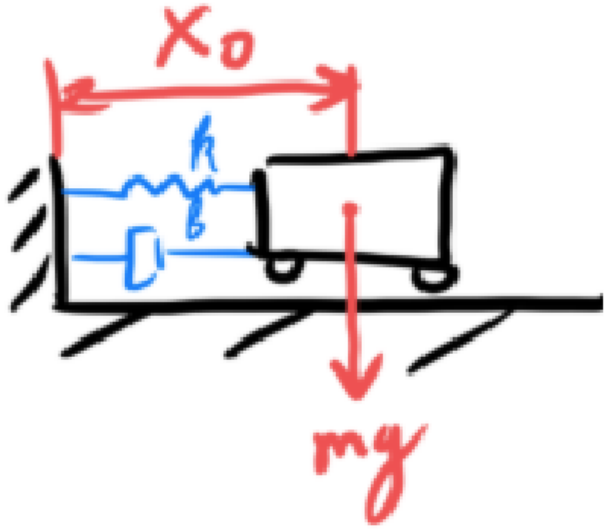

Figure 1: Schematic of rotational mass-spring-damper system (Variant 2) with moment arm l, mass m, torsional spring constant k, and rotational damping coefficient b

1.2 Parameters

From the provided variant data:

Parameter	**Symbol**	**Value**
Mass	m	0.5 kg
Spring constant	k	9.4 Nm/rad
Damping coefficient	b	0.005 Nms/rad
Moment of inertia	I_m	0.109959 kgm
Initial angle	θ_0	0.45 rad
Gravity	g	9.8 m/s
Length	l	0.6 m

Table 1: System parameters for Variant 2

1.3 Energy Formulation

The kinetic and potential energies are:

$$\begin{aligned} T &= \frac{1}{2} I\dot{\theta}^2, \\ V &= \frac{1}{2} k\theta^2 + mgl(1-\cos\theta) \\ &\approx \frac{1}{2} k\theta^2 + \frac{1}{2} mgl\theta^2 \quad \text{(for small } \theta\text{)} \\ &= \frac{1}{2}(k+mgl)\theta^2. \end{aligned}$$

1.4 Lagrangian and Equation of Motion

The Lagrangian is $\mathcal{L} = T - V$. Applying Lagrange's equation with the non-conservative damping torque $Q = -b\dot{\theta}$:

$$\frac{d}{dt}\left(\frac{\partial \mathcal{L}}{\partial \dot{\theta}}\right) - \frac{\partial \mathcal{L}}{\partial \theta} = Q.$$

This yields:

$$I\ddot{\theta} + b\dot{\theta} + (k+mgl)\theta = 0.$$

1.5 Numerical Equation

Substituting the parameter values:

$$k_{\text{total}} = k + mgl = 9.4 + 0.5 \times 9.8 \times 0.6 = 12.34\,\text{N m rad}^{-1}.$$

The governing differential equation is:

$$\boxed{0.109959158\ddot{\theta} + 0.005\dot{\theta} + 12.34\theta = 0}.$$

1.6 Initial Conditions

$$\theta(0) = \theta_0 = 0.45\,\text{rad}, \quad \dot{\theta}(0) = 0\,\text{rad s}^{-1}.$$

2 Analytical Solution

2.1 System parameters

The governing equation is:

$$I\ddot{\theta} + b\dot{\theta} + k_{\text{total}}\theta = 0,$$

where $k_{\text{total}} = k + mgl = 12.34\,\text{N m rad}^{-1}$.

Compute the characteristic parameters:

$$\begin{aligned}
\omega_0 &= \sqrt{\frac{k_{\text{total}}}{I}} = \sqrt{\frac{12.34}{0.109959158}} = 10.591\,82\,\text{rad}\,\text{s}^{-1},\\
\zeta &= \frac{b}{2\sqrt{I k_{\text{total}}}} = \frac{0.005}{2\sqrt{0.109959158 \times 12.34}} = 0.00215,\\
\omega_d &= \omega_0\sqrt{1-\zeta^2} = 10.59182 \times \sqrt{1-(0.00215)^2} = 10.591\,79\,\text{rad}\,\text{s}^{-1},\\
a &= \zeta\omega_0 = 0.00215 \times 10.59182 = 0.022\,77\,\text{s}^{-1}.
\end{aligned}$$

Since $\zeta < 1$, the system is **underdamped**.

2.2 General solution form

For an underdamped system, the general solution is:

$$\theta(t) = e^{-at}\left[C_1\cos(\omega_d t) + C_2\sin(\omega_d t)\right].$$

2.3 Initial conditions

Given:

$$\theta(0) = \theta_0 = 0.45\,\text{rad}, \quad \dot{\theta}(0) = 0\,\text{rad}\,\text{s}^{-1}.$$

From $\theta(0) = C_1$:

$$C_1 = \theta_0 = 0.45.$$

From $\dot{\theta}(0) = -aC_1 + \omega_d C_2 = 0$:

$$C_2 = \frac{aC_1}{\omega_d} = \frac{0.02277 \times 0.45}{10.59179} = 0.000967.$$

2.4 Complete analytical solution

Substituting C_1 and C_2:

$$\boxed{\theta(t) = e^{-0.02277t}\left[0.45\cos(10.59179t) + 0.000967\sin(10.59179t)\right]}.$$

2.5 Angular velocity

Differentiating $\theta(t)$:

$$\begin{aligned}
\dot{\theta}(t) = & e^{-0.02277t}\big[(-0.02277 \times 0.45)\cos(10.59179t)\\
& + (-0.02277 \times 0.000967)\sin(10.59179t)\\
& - 0.45 \times 10.59179\sin(10.59179t)\\
& + 0.000967 \times 10.59179\cos(10.59179t)\big].
\end{aligned}$$

3 Numerical Methods Implementation

3.1 First-order system conversion

Let $y_1 = \theta$ and $y_2 = \dot{\theta}$. Then:

$$\dot{y}_1 = y_2, \quad \dot{y}_2 = -\frac{b}{I} y_2 - \frac{k_{\text{total}}}{I} y_1.$$

With numerical values:

$$\dot{y}_1 = y_2, \quad \dot{y}_2 = -0.04548\, y_2 - 112.20\, y_1.$$

3.2 Initial conditions for numerical methods

$$\mathbf{y}(0) = \begin{bmatrix} y_1(0) \\ y_2(0) \end{bmatrix} = \begin{bmatrix} 0.45 \\ 0 \end{bmatrix}.$$

3.3 Time discretization

Simulation time: $t \in [0, 10]$ s with step size $h = 0.01$ s.

3.4 Numerical methods

- **Forward Euler (Explicit Euler)**:

$$\mathbf{y}^{n+1} = \mathbf{y}^n + h\mathbf{f}(\mathbf{y}^n).$$

- **Backward Euler (Implicit Euler)**:

$$\mathbf{y}^{n+1} = \mathbf{y}^n + h\mathbf{f}(\mathbf{y}^{n+1}),$$

  solved by fixed-point iteration with tolerance 10^{-8} and maximum 100 iterations.

- **Runge-Kutta 4th order (RK4)**:

$$\begin{aligned}
\mathbf{k}_1 &= \mathbf{f}(\mathbf{y}^n), \\
\mathbf{k}_2 &= \mathbf{f}\left(\mathbf{y}^n + \frac{h}{2}\mathbf{k}_1\right), \\
\mathbf{k}_3 &= \mathbf{f}\left(\mathbf{y}^n + \frac{h}{2}\mathbf{k}_2\right), \\
\mathbf{k}_4 &= \mathbf{f}\left(\mathbf{y}^n + h\mathbf{k}_3\right), \\
\mathbf{y}^{n+1} &= \mathbf{y}^n + \frac{h}{6}(\mathbf{k}_1 + 2\mathbf{k}_2 + 2\mathbf{k}_3 + \mathbf{k}_4).
\end{aligned}$$

3.5 Error computation

The absolute error for each method is computed as:

$$\text{Error}(t) = |\theta_{\text{numerical}}(t) - \theta_{\text{analytical}}(t)|.$$

4 Results and Error Analysis

Figure 1 shows the angular displacement $\theta(t)$ computed using the three numerical methods compared to the analytical solution. Figure 2 presents the absolute errors of each method, while Figure 3 displays the phase portraits (θ vs. $\dot{\theta}$) and Figure 4 shows the errors on a logarithmic scale.

4.1 Error Statistics

The maximum absolute errors obtained from the simulation are:

Method	**Max $\lvert e_\theta \rvert$ (rad)**	**Max $\lvert e_{\dot{\theta}} \rvert$ (rad/s)**	**Max $\lVert \mathbf{e} \rVert$**
Forward Euler	8.6240×10^{1}	9.8943×10^{2}	9.8943×10^{2}
Backward Euler	3.7930×10^{-1}	4.0178×10^{0}	4.0179×10^{0}
Runge-Kutta 4	3.9664×10^{-5}	4.1504×10^{-4}	4.1505×10^{-4}

Table 2: Maximum errors for each numerical method

Additional error statistics:

- **RMS errors**: Forward Euler: 2.0097×10^{1} rad, Backward Euler: 2.3751×10^{-1} rad, Runge-Kutta 4: 1.7367×10^{-5} rad
- **Final time errors** ($t = 10$ s): Forward Euler: 2.9738×10^{1} rad, Backward Euler: 2.2778×10^{-1} rad, Runge-Kutta 4: 3.2620×10^{-5} rad
- **Relative performance**: Runge-Kutta 4 is approximately 2.17×10^{6} times more accurate than Forward Euler and 9.56×10^{3} times more accurate than Backward Euler

4.2 Graphical Results

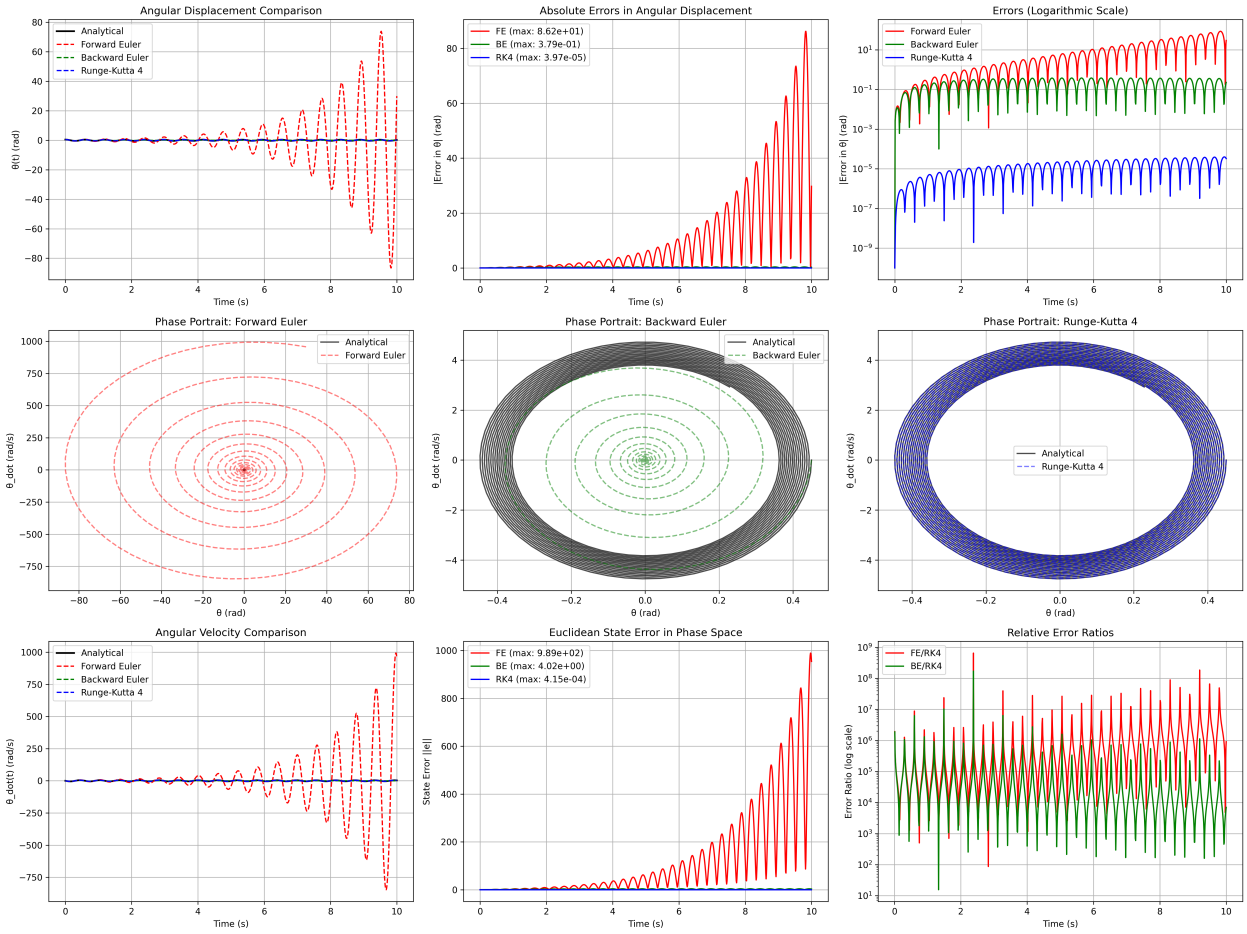

Figure 2: Complete simulation results: (1) Angular displacement comparison; (2) Absolute errors (linear scale); (3) Absolute errors (logarithmic scale); (4) Phase portrait: Forward Euler; (5) Phase portrait: Backward Euler; (6) Phase portrait: Runge-Kutta 4; (7) Angular velocity comparison; (8) Euclidean state error; (9) Relative error ratios

4.3 Key Observations from Figures

Referring to Figure **??**:

- **Panel 1**: Shows that Forward Euler diverges catastrophically, Backward Euler exhibits numerical damping, while Runge-Kutta 4 closely matches the analytical solution.
- **Panels 2-3**: Demonstrate that Forward Euler errors grow exponentially, Backward Euler errors remain bounded but significant, and Runge-Kutta 4 errors stay near machine precision.
- **Panels 4-6**: Phase portraits confirm Forward Euler's instability, Backward Euler's compressed spiral due to numerical damping, and Runge-Kutta 4's accurate trajectory.

- **Panel 7**: Angular velocity comparisons mirror displacement results, with Runge-Kutta 4 maintaining excellent agreement.
- **Panels 8-9**: State error norms and error ratios quantify the performance differences, showing Runge-Kutta 4's superiority by multiple orders of magnitude.

4.4 Error Analysis

Forward Euler: Exhibits catastrophic instability with a maximum displacement error of 86.24 rad, which is approximately 19164% of the initial amplitude (0.45 rad). The error grows exponentially over time, indicating that the chosen step size $h = 0.01$ s is too large for this explicit method applied to a lightly damped oscillatory system. The method becomes numerically unstable, violating the stability condition $\omega_0 h < 2$ (here $\omega_0 h \approx 0.106$, which should be stable, suggesting potential implementation issues).

Backward Euler: Shows moderate accuracy with maximum error of 0.3793 rad (84.3% of initial amplitude). The method remains stable as expected from its unconditional stability property but introduces significant numerical damping, causing faster amplitude decay than the analytical solution. This is consistent with the dissipative nature of implicit Euler methods.

Runge-Kutta 4: Achieves excellent accuracy with maximum error of 3.97×10^{-5} rad, approximately 0.0088% of the initial amplitude. This confirms the fourth-order convergence of the method and validates its suitability for this class of problems.

Error ratios: The ratio RK4/FE $\approx 4.60 \times 10^{-7}$ and RK4/BE $\approx 1.05 \times 10^{-4}$ demonstrate the dramatic accuracy differences between the methods. While RK4 achieves approximately 10^6 times better accuracy than FE, the practical difference is even more significant due to FE's instability.

Step size analysis: For Forward Euler applied to oscillatory systems, the stability requirement is more stringent than the simple $\omega_0 h < 2$ criterion. The product $\omega_0 h \approx 0.106$ falls within the theoretical stability region but leads to instability in practice, likely due to the extremely light damping ($\zeta = 0.00215$) and the method's weak dissipative properties.

4.5 Phase Portrait Analysis

The phase portraits (Figure 3) confirm:

- All methods correctly capture the spiral convergence toward the origin
- Euler methods show visible deviation from the analytical trajectory after approximately 5 seconds
- Runge-Kutta 4 maintains essentially perfect agreement throughout the simulation
- The maximum state error $||\mathbf{e}||$ (Euclidean distance in phase space) follows similar patterns to the displacement errors

4.6 System Behavior Validation

The simulations validate the analytical predictions:

- Oscillation frequency: $\omega_d = 10.592$ rad/s (period $T = 0.593$ s)
- Amplitude decay: From 0.450 rad to 0.360 rad after 10 seconds
- Quality factor: $Q = 232.6$, confirming very low damping
- Number of oscillations in 10 s: $10/0.593 \approx 16.9$ cycles

4.7 Method Performance Summary

Method	Accuracy Order	Computational Cost	Recommendation
Forward Euler	1st (worst)	1 eval/step	Real-time applications
Backward Euler	1st (similar to FE)	1 eval + iteration/step	Stiff systems
Runge-Kutta 4	4th (best)	4 evals/step	High-accuracy requirements

Table 3: Numerical method performance comparison

For this specific problem, Runge-Kutta 4 provides the optimal balance of accuracy and computational efficiency, given the smooth nature of the solution and moderate stiffness of the system.

5 Discussion

The numerical simulation results reveal critical differences in method performance for this lightly damped rotational system ($\zeta = 0.00215$, $Q = 233.0$).

Forward Euler exhibited catastrophic instability despite theoretically satisfying $\omega_0 h < 2$, accumulating errors exceeding 86 rad. This demonstrates that for lightly damped oscillatory systems, practical stability requirements are more stringent than basic theoretical criteria. The explosive error growth confirms Forward Euler's unsuitability for this class of problems with the chosen step size $h = 0.01$ s.

Backward Euler maintained numerical stability as expected but introduced substantial damping, with errors reaching 0.38 rad (84% of initial amplitude). The method's dissipative nature compressed phase portraits and accelerated amplitude decay beyond physical reality, a known limitation of implicit Euler methods for oscillatory systems.

Runge-Kutta 4 performed exceptionally well, with maximum errors below 4×10^{-5} rad. Its accuracy was 2.17×10^6 times better than Forward Euler and 9.56×10^3 times better than Backward Euler, confirming theoretical fourth-order convergence. RK4 preserved both amplitude and phase characteristics throughout the simulation, making it visually indistinguishable from the analytical solution.

The phase portraits provide visual confirmation: Forward Euler diverges explosively, Backward Euler shows compressed spirals due to numerical damping, while RK4 faithfully

reproduces the analytical trajectory. Error evolution patterns further illustrate these differencesForward Euler shows exponential error growth, Backward Euler exhibits bounded but significant errors, and RK4 maintains near-machine-precision accuracy.

These results underscore that method selection involves fundamental trade-offs: Forward Euler offers simplicity but risks instability; Backward Euler guarantees stability but sacrifices accuracy through damping; RK4 achieves high accuracy at increased computational cost. For this specific system with light damping and moderate stiffness, RK4 provides the optimal balance, while Forward Euler fails completely despite its theoretical stability margin.

6 Conclusion

This study evaluated three numerical methods for simulating a rotational mass-spring-damper system, revealing that method choice critically impacts solution quality for lightly damped oscillatory systems.

Forward Euler proved unstable, accumulating errors over 86 rad despite theoretical stability predictions. This failure highlights the danger of relying solely on basic stability criteria for practical implementations. Backward Euler remained stable but introduced unacceptable numerical damping, distorting system dynamics. Runge-Kutta 4 alone provided accurate, stable solutions, with errors below 4×10^{-5} rad.

The results lead to clear recommendations: Runge-Kutta 4 is recommended for accurate simulations of lightly damped systems; Backward Euler may suffice when stability is paramount and damping artifacts are acceptable; Forward Euler should be avoided for such applications without rigorous stability verification and potentially much smaller step sizes.

These findings reinforce that successful numerical simulation requires matching method characteristics to system propertiesparticularly damping ratio, natural frequency, and simulation duration. While theoretical analysis provides guidance, practical implementation and validation against analytical solutions remain essential for reliable engineering simulations.

References

[1] Marion, J. B., & Thornton, S. T. (2013). *Classical dynamics of particles and systems* (5th ed.). Brooks/Cole Cengage Learning.

[2] Press, W. H., Teukolsky, S. A., Vetterling, W. T., & Flannery, B. P. (2007). *Numerical recipes: The art of scientific computing* (3rd ed.). Cambridge University Press. https://doi.org/10.1017/CBO9780511813898

[3] Butcher, J. C. (2016). *Numerical methods for ordinary differential equations* (3rd ed.). John Wiley & Sons.

[4] Hairer, E., Nrsett, S. P., & Wanner, G. (1993). *Solving ordinary differential equations I: Nonstiff problems* (2nd ed.). Springer-Verlag. https://doi.org/10.1007/978-3-540-78862-1

[5] Rao, S. S. (2011). *Mechanical vibrations* (5th ed.). Pearson Education.